energies

MDPI

Article

Experimental Study on a Novel Form-Stable Phase Change Material Based on Solid Waste Iron Tailings as Supporting Material for Thermal Energy Storage

Peng Liu [1,2,3], Yajing Wang [1,2,3,*], Zhao Liang [4], Zhikai Zhang [5], Jun Rao [1,2,3] and Shuai Jiang [6]

1 School of Gems and Materials Technology, Hebei Geo University, Shijiazhuang 050031, China
2 Engineering Research Center for Silicate Solid Waste Resource Utilization of Hebei Province, Shijiazhuang 050031, China
3 Hebei Key Laboratory of Green Development of Rock and Mineral Materials of Hebei Province, Shijiazhuang 050031, China
4 Science and Technology Department, Hebei GEO University, Shijiazhuang 050031, China
5 School of Water Resources and Environment, Hebei GEO University, Shijiazhuang 050031, China
6 Shengli Xinda New Material Company Ltd., Dongying 257000, China
* Correspondence: wyjbs@hgu.edu.cn

Abstract: To prevent liquid leakage during the phase transition of a phase change material (PCM), a novel form-stable PCM (FSPCM) based on LA/CIT/CNT was fabricated using a simple and facile direct impregnation method. The iron tailings (ITs) was calcinated at first. And then lauric acid (LA) was impregnated into the calcinated iron tailings (CITs) with carbon nanotubes (CNTs) as a thermal conductivity additive. Subsequently, the leakage tests and the properties of the prepared samples were investigated by diffusion-oozing testing (DOT), SEM, XRD, FTIR, DSC, TGA, and intelligent paperless recorder (IPR). DOT results showed that the impregnation ratio of LA into the CIT and CNT was up to 27.5% without leakage. SEM indicated that LA can be adsorbed into microscale pores and covered the surface of CITs and CNTs. FTIR spectra indicated that there was no chemical reaction during the preparation process. The melting and freezing temperatures of the prepared LA/CIT/CNT FSPCMs were measured as 45.24 °C and 39.61 °C, respectively. Correspondingly, the latent heat values were determined as 39.95 J/g and 35.63 J/g, respectively. The LA/CIT/CNT FSPCMs exhibited good thermal stability in the working temperature range, and its heat transfer efficiency was improved significantly by 69.23% for LA and 84.62% for LA/CIT FSPCM. In short, LA/CIT/CNT FSPCMs are a very promising material for thermal energy storage in practical low-temperature applications.

Keywords: lauric acid; calcinated iron tailings; carbon nanotubes; FSPCM; low-temperature thermal energy storage

Citation: Liu, P.; Wang, Y.; Liang, Z.; Zhang, Z.; Rao, J.; Jiang, S. Experimental Study on a Novel Form-Stable Phase Change Material Based on Solid Waste Iron Tailings as Supporting Material for Thermal Energy Storage. *Energies* **2023**, *16*, 7037. https://doi.org/10.3390/en16207037

Academic Editors: Philippe Leclère, Tapas Mallick and F. Pacheco Torgal

Received: 30 June 2023
Revised: 23 August 2023
Accepted: 28 September 2023
Published: 11 October 2023

1. Introduction

It is well known that the development and utilization of renewable energy have been given worldwide attention due to the shortage of fossil energy and environmental pollution caused by fossil energy [1,2]. However, the shortcomings of poor utilization efficiency and bad supply stability seriously limit the large-scale practical application of renewable energy. The imbalance between energy supply and demand is forcing people to develop various new energy storage technologies [3,4]. Fortunately, the phase change material (PCM), as a key factor in thermal storage technology (TES), is becoming an efficient and clean method to solve the problems mentioned above due to its many advantages, such as high latent heat capacity, low price, and incombustibility [5–7]. Among the PCMs researched, fatty acids, such as lauric acid (LA), are considered to be very promising PCMs in TES because they show obvious advantages, such as low cost, high latent heat of fusion, small volume change during solid–liquid phase transition, low supercooling degree, ready

availability, non-flammable, good compatibility and thermal stability, non-toxicity, low vapor pressure, non-corrosiveness and particularly suitable phase-change temperature that make it preferable for the intended low-temperature application [8,9]. However, their practical applications are restricted due to poor thermal conductivity and leakage during the phase transition [1,4]. Hence, it is urgent to overcome the two shortcomings of fatty acids, into which a lot of effort has been put by many researchers. On one hand, it has been confirmed that high thermal conductivity additives could simply and effectively enhance fatty acids' thermal conductivity [4]. For example, carbon nanotubes (CNTs) are currently considered to be one of several relatively ideal additives owing to its high specific surface area, thermal conductivity, and low weight [10,11]. On the other hand, employing a supporting matrix to adsorb fatty acids onto porous minerals to fabricate FSPCMs is regarded as an effective, low-cost, and simple method to solve the leakage problem [12,13]. The investigated porous minerals include perlite [14,15], kaolinite [16,17], diatomite [18,19], expanded graphite [13,20], and so on. However, most raw porous minerals are exhaustive, relatively exiguous, and costly. Therefore, it is very necessary to study a large quantity of low-cost, alternative, porous materials.

Interestingly, it is worth noting that iron tailings (ITs), as the by-product of iron ore separation, has obvious characteristics of being considerably cheap, quite easily available, and in large amounts, making it convenient for large-scale production and application. Furthermore, ITs occupy a very large part of industrial solid wastes, and the treatment and recycling utilization of ITs has always been a problem all over the world [21–23]. Fortunately, the main chemical components of ITs are similar to several natural mineral materials reported in the literature [16,18,24–29]. Based on the fundamental knowledge, it is possible to utilize ITs as a supporting matrix to restrict the leakage of fatty acids. There have been several reports on the exploration and research of composite phase change materials based on ITs. However, composite PCMs with different component systems have different characteristics and thermal and physical properties [4,30]. Employing IT as the support material of PCM can effectively prevent the liquid leakage of LA and facilitate the coupling of PCM with building materials. Therefore, in this study, IT was first calcinated to improve the loading capacity of the LA. Then, LA, calcinated ITs (CITs) and CNTs were used as PCM, supporting matrix, and thermal conductivity additive, respectively. A novel form-stable phase change material (FSPCM) of LA/CIT/CNT was fabricated via simple and facile direct impregnation. Subsequently, the leakage testing, physical structure, and thermal properties were systemically studied by diffusion-oozing testing (DOT), scanning electron microscopy (SEM), Fourier transform infrared (FTIR), differential scanning calorimeter (DSC), thermal gravimetric analysis (TGA), and intelligent paperless recorder (IPR). Using ITs as a support material for PCMs could not only prevent PCM leakage from occurring in FSPCM, but also provide a new technological approach for the high-value utilization of IT and further improve its resource utilization level.

2. Experiment

2.1. Materials

The LA was provided by Shanghai Sinopharm Chemical Reagent Co., Ltd., Shanghai, China. The ITs were collected from the Hebei Hanxing Mining Bureau, Handan, China, whose chemical components are given in Table 1. The CNTs were obtained from Suzhou Tanfeng Tech. Inc. Reagent Co., Ltd., Suzhou, China. The montmorillonite binder additive was supplied by Yipusheng Tianjin Pharmaceutical Co., Ltd, Tianjin, China.

Table 1. Comparisons of chemical constituent of ITs and CITs [31].

Material	SiO_2	Al_2O_3	Fe_2O_3	CaO	MgO	$K_2O + Na_2O$	Others
IT	31.98	6.49	10.23	30.77	13.84	1.64	5.05
CIT	33.97	7.23	10.59	31.14	13.91	1.66	1.50

2.2. Preparation of FSPCM

The LA/CIT/CNT FSPCMs were synthesized by simple and facile direct impregnation [1,4,32]. The whole preparation procedure of the LA/CIT/CNT composites is illustrated in Figure 1. Firstly, the ITs were screened into −60 mesh before use, and then mixed with montmorillonite binder additive. Afterward the mixture was calcinated at 300 °C for half an hour in a high-temperature furnace. Then, the mixture was again heated constantly at 600 °C for 2 h. After that, the residual ash was cooled to 20 °C [31–33]. Thus CIT can be obtained, and its chemical components are also shown in Table 1. The comparison of chemical components between CIT and IT in Table 1 demonstrated that IT can be employed as a supporting matrix to prevent leakage of LA in theory. Subsequently, the specified amount of LA and CIT were weighed and mixed according to different mass fractions in 250 mL beakers, respectively. The mixture was heated in a water bath, and the temperature of the water bath was maintained at 75 °C for 20 min. Meanwhile, the mixture was continuously stirred using a glass rod by hand. Then, the obtained LA/CIT composites were cooled to room temperature. And the LA/CIT composites were achieved. Secondly, according to the literature [1,32,34], the leakage tests were performed on the magnetic stirrers by using the DOT method at 60 °C, respectively. Like this, the composite without leakage of LA was called FSPCM. Thirdly, CNTs with different mass fractions of 1, 3, 5, and 7% were added into the LA/CIT FSPCM to fabricate the LA/CIT/CNT FSPCM. And the experimental conditions and procedures mentioned above were repeated. Thus, the LA/CIT/CNT FSPCM was obtained.

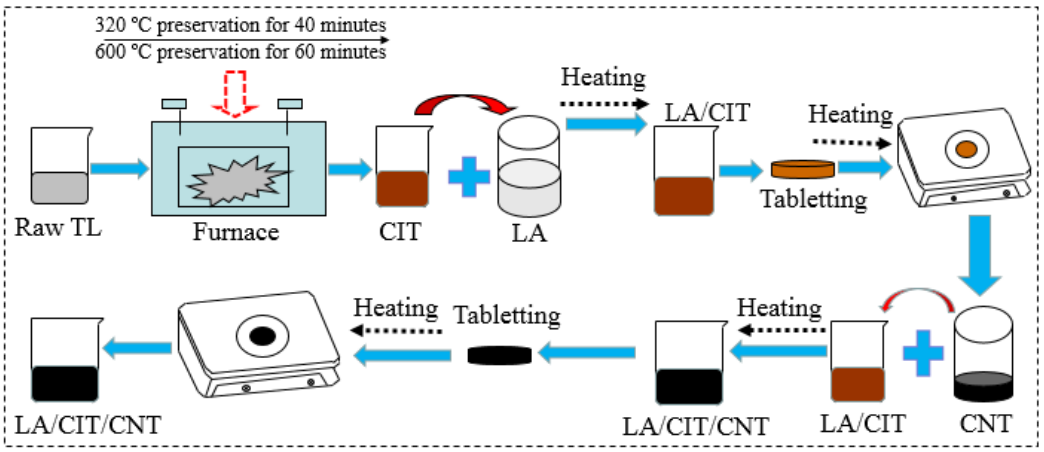

Figure 1. Preparation procedures of LA/CIT/CNT FSPCM.

2.3. Characterization of FSPCMs

The microstructure morphology of LA, CITs, CNTs, LA/CIT FSPCMs, and LA/CIT/CNT FSPCMs were researched by SEM. The FTIR spectra with a resolution of 2 cm^{-1} were recorded to investigate the chemical compatibility between the components of the FSPCMs at a wavenumber range of 400–4000 cm^{-1}. The thermal properties of FSPCMs were studied by DSC at a heating rate of 10 °C/min in a N_2 atmosphere. The latent heat accuracy and phase change temperature deviation were of the DSC 0.1% and 0.1 °C, respectively. The thermal stability of LA and the FSPCMs were investigated by TGA at 25–400 °C with a heating rate of 20 °C/min under a N_2 atmosphere. The heat transfer efficiency of the FSPCMs was analyzed by IPR at the temperature range from 20 °C to 75 °C for the heating process and 75 °C to 20 °C for the freezing process, respectively. Moreover, the leakage area and leakage ratio were used to examine the leakage of composites. The leakage area was acquired while referring to the literature [35]. The leakage area was calculated according to the average diameter of three measurement results of each sample measured by a ruler with a test error of ±0.5 mm in eight directions. And the leakage ratio was calculated according to Ramakrishnan [36]. The leakage ratio was the mass of leaked LA divided by

the total mass of LA in the corresponding composites. The evaluation results were also listed in Table 2.

Table 2. Basic proportion and leakage results of the prepared composites.

Sample	LA	CIT	CNT	Leakage Area of Samples (cm^2)	Leakage Ration (%)
S1-1	5	5	0	88.25	19.6
S1-2	4	6	0	65.04	12.4
S1-3	3	7	0	33.18	3.83
S1-4	2	8	0	0	0
S2-1	2.75	7.25	0	19.63	2.433
S2-2	2.5	7.5	0	12.25	1.233
S2-3	2.25	7.75	0	—	0.1
S2-4	3	7	1	—	0.4
S3-1	2.75	7.25	1	—	0.23
S3-2	2.75	7.25	3	0	0
S3-3	2.75	7.25	5	0	0
S3-4	2.75	7.25	7	0	0

3. Results and Discussion

3.1. Leakage Phenomenon and Leakage Evaluation

The leakage testing results of the composites are described in Figures 2 and 3. The quantitative results are also listed in Table 2. As described in Figure 2 and Table 2, the deformation of the composite from S1-4 to S1-1 in Figure 2 became more and more serious with the decreasing mass fraction of CIT. That is to say, the leakage of LA within the corresponding composites became weaker and weaker from S1-1 to S1-4, as shown in Figure 4, with the mass fraction of CITs increasing. Moreover, when the mass fraction of CITs in composite was about 20%, the corresponding composite can keep a preferable stable state without the leakage of LA. Namely, the composite S1-4 in Figure 2 could successfully restrict the leakage of LA, which indicated this composite could be called FSPCM. Therefore, to determine the relatively superior mass ratio between LA and CITs, the leakage tests were carried out with subdivided a mass ratio ranging from 3:7 to 2:8 between LA and CITs. The testing results are also given in Figure 2 and Table 2. Though the composite S2-1, S2-2, and S2-3 showed good form stability, LA stains were noticeable around the S2-1, S2-2, and S2-3 discs on the filter papers, respectively, indicating that LA leakage occurred in S2-1, S2-2, and S2-3. Therefore, to improve the package efficiency and heat transfer efficiency, the porous and high thermal conductivity CNTs were used as a heat transfer enhancer. The leakage test of the LA/CIT/CNT (1%) sample (S2-4) was first carried out with a CNT mass fraction of 1%, and the mass ratio of LA and CIT at 3:7. The testing result is also given in Figure 2. It can be seen that S2-4 left stains on the filter paper, which revealed that the LA/CIT/CNT (1%) sample with mass ratio at 3:7 between LA and CIT was not suitable as a kind of FSPCM. Therefore, the leakage tests of LA/CIT/CNT samples were also investigated when the LA-to-CIT mass ratio was at 2.75:7.25 and the CNT mass fractions were 1%, 3%, 5%, and 7%, respectively. The testing results were shown in Figure 3. As seen from Figure 3, the LA/CIT/CNT samples of mass ratio 2.75:7.25 between LA and CIT not only maintained form stability, but there were also no stains on the filter papers. This indicated that the addition of CNTs can further help to enhance the packaging efficiency of LA and consequently increase the latent heat of FSPCMs in later thermal storage property tests. In a word, with comprehensive consideration of packaging efficiency and heat transfer efficiency, the LA/CIT/CNT (3%) of mass ratio of 2.75:7.25 between LA and CITs was determined as the FSPCM samples in the following work. Additionally, as can be seen from Table 2, the leakage area and leakage ratio can relatively intuitively, quantitatively, and objectively describe the deformation and leakage of the composite, respectively. The leakage phenomenon and leakage results in Table 2 are consistent with the results in Figures 2 and 3.

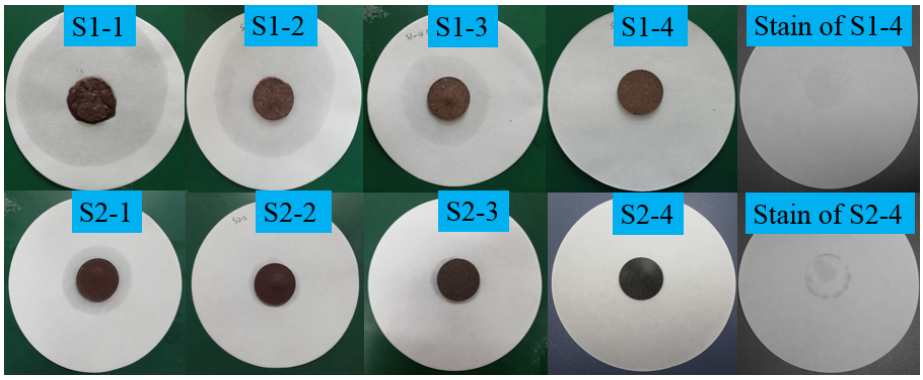

Figure 2. Leakage results obtained after heating at 60 °C of LA/CIT composites.

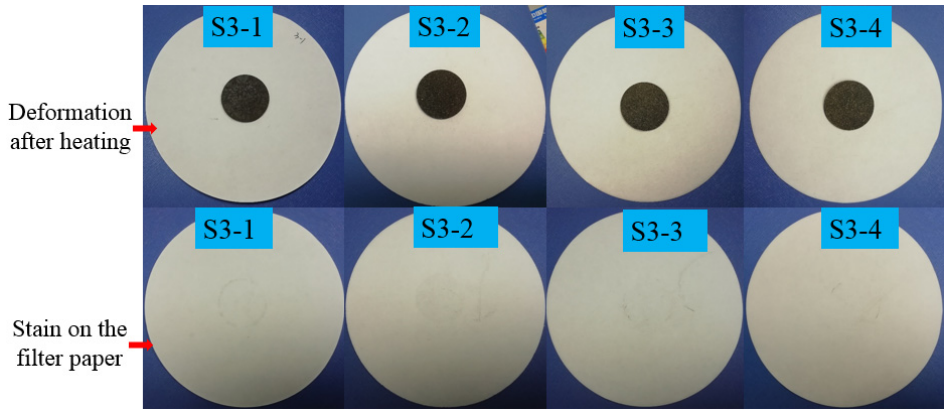

Figure 3. Leakage results and liquid stains on the paper after heating at 60 °C of LA/CIT composites of S3-1, S3-2, S3-3, and S3-4.

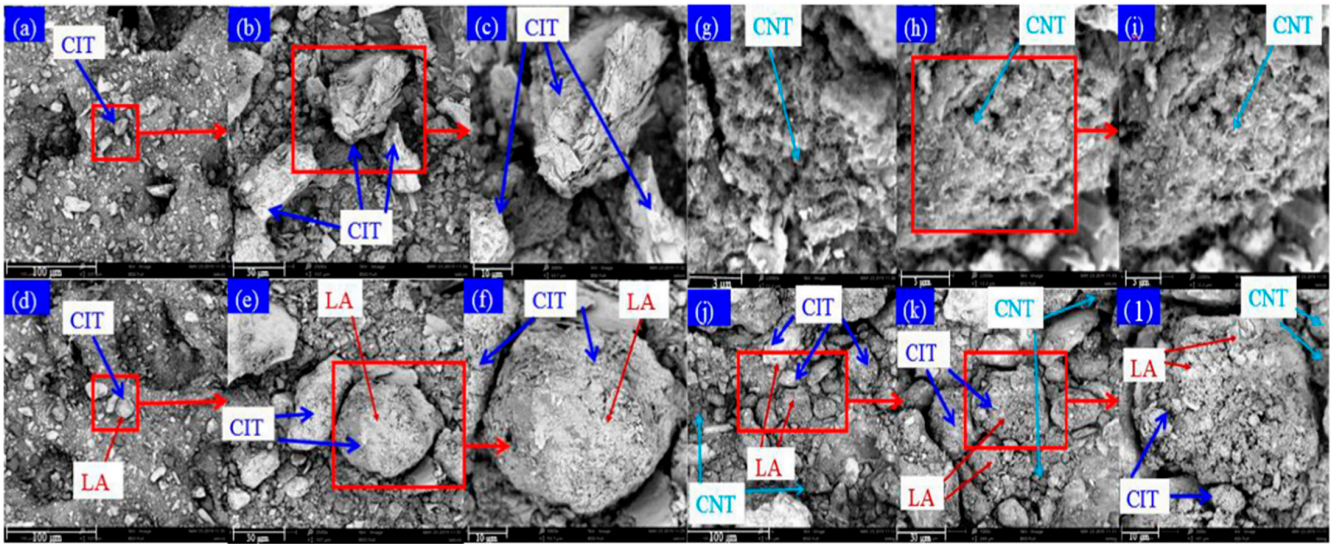

Figure 4. SEM photographs of CIT (**a**–**c**), LA/CIT (**d**–**f**), CNT (**g**–**i**), LA/CIT/CNT (**j**–**l**).

3.2. Morphology and Microstructure of FSPCMS

The morphology of CITs, CNTs, LA/CIT FSPCMs, and LA/CIT/CNT FSPCMs are presented in Figure 4. It can be seen that CITs possessed numerous rugged porous holes microstructure, as revealed in Figure 4a–c. Figure 4d–f showed that the CITs' surface was completely covered by the adsorbed LA due to capillary and surface tension forces. Meanwhile, after LA was incorporated into CIT, the micro-porous structure on the CITs'

surface disappeared, indicating that more LA can be adsorbed. And the surface of CIT became smooth, which demonstrated that LA was fully absorbed into the rugged microporous and covered the surface of the CITs. That is to say, CITs can restrict the leakage of liquid LA, while CNTs had various pore network structures like clustered cotton wool, as indicated in Figure 4g–i. Moreover, Figure 4j–l illustrates that some CNTs or CNTs mixed with liquid LA were dispersed into the micro-pores of CITs and covered the surface, which reflected that the CNTs were successfully impregnated into the synthesized FSPCM, whereas other CNTs or CNTs mixed with liquid LA distributed the space among CIT particles, which objectively provided a path channel to enhance the heat transfer efficiency of LA.

3.3. Chemical Compatibility of FSPCMs

The FTIR spectra of LA, TL, CITs, and the prepared FSPCMs are presented in Figure 5. In the spectrum of LA, there were five major absorption peaks observed, as shown in Figure 5. The absorption peak of the in-plane swinging vibration and out-of-plane bending vibration of -OH was found at 937 cm^{-1} and 723 cm^{-1}, respectively. The absorption peak at 1704 cm^{-1} represented the stretching vibration of the C=O group. The absorption peaks of the stretching variation of the C–H bond in the $–CH_2$ and $–CH_3$ function groups were found at 2923 cm^{-1} and 2853 cm^{-1}, respectively [37,38]. In the spectrum of CITs, the stretching vibration peaks caused by the Si–O–Si group appeared at 476, 695, and 882 cm^{-1}. And the Si–O group stretching vibrations were observed at 1090 and 1170 cm^{-1} [31]. In the spectra of the prepared FSPCMs, all of the major characteristic peaks overlapped with those of the three components, namely, LA, CITs, and CNTs. Furthermore, compared to the pure LA, the non-existence of new vibration peaks indicated no chemical reaction occurred among LA, CITs, and CNTs. The FTIR analysis demonstrated that the prepared LA/CIT/CNT FSPCMs had excellent chemical compatibility.

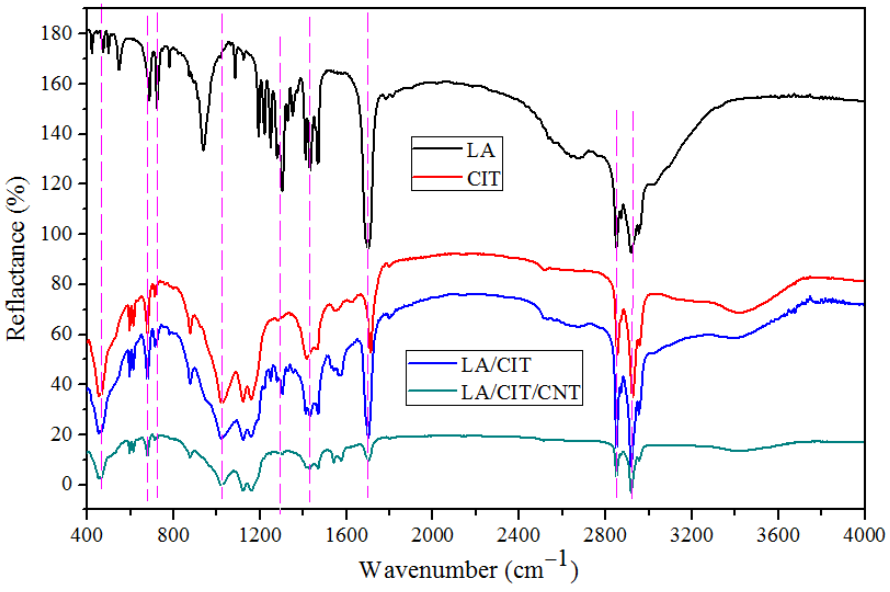

Figure 5. FTIR spectra of LA, TL, CIT, LA/CIT, and LA/CIT/CNT samples.

3.4. Thermal Properties of the FSPCMs

Thermal energy storage performances gained by DSC of LA and the LA/CIT FSPCMs and LA/CIT/CNT FSPCMs are described in Figure 6. The detailed data were listed in Table 3. The phase-change temperatures of LA, LA/CIT FSPCM, and LA/CIT/CNT FSPCM were about 46.46 °C, 45.8 °C, and 45.24 °C during storage and 41.23 °C, 39.39 °C, and 39.61 °C during discharging, respectively. The phase-change temperatures of the fabricated FSPCMs were slightly lower than those of LA (changed slightly) due to the confinement of

LA in the micro-pores of CITs. The latent heat values of LA and the LA/CIT FSPCMs and LA/CIT/CNT FSPCMs were about 182.6 J/g, 45.06 J/g, and 39.95 J/g when charging and 181.4 J/g, 38.73 J/g, and 35.63 J/g when discharging, respectively. The latent heat values of the LA/CIT FSPCMs and LA/CIT/CNT FSPCMs were lower than that of pure LA due to the interference of CITs, which affected on the crystal arrangement and the orientation of the molecules chains of LA.

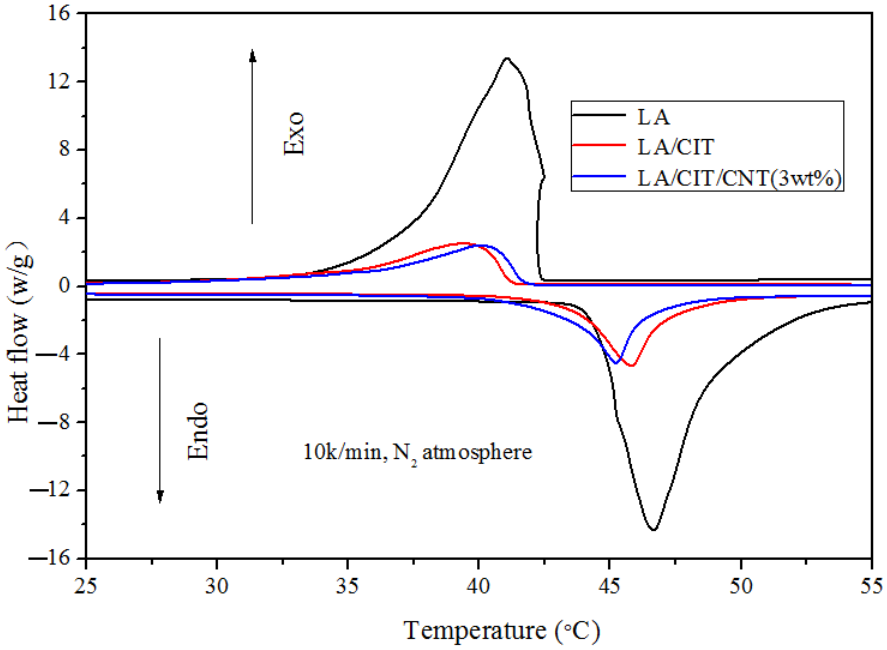

Figure 6. DSC cures of LA, LA/CIT FSPCMs and LA/CIT/CNT FSPCMs.

Table 3. Thermal properties of the synthesized samples.

Samples	Loading of LA (%)	Melting Temperature (°C)	Solidifying Temperature (°C)	Measured Latent Heat of Melting (J/g)	Measured Latent Heat of Solidifying (J/g)
LA	100	46.46	41.23	182.6	181.4
LA27.5%/CIT	24.68	45.8	39.39	45.06	38.73
LA27.5%/CIT/CNT3%	21.88	45.24	39.61	39.95	35.63

Table 4 shows the comparison of thermal properties between this work and others in the literature. It can be seen from Table 4 that the latent heat value of the LA/CIT/CNT FSPCMs was higher than that of other composites in the literature by using other supporting matrices. Namely, the LA/CIT/CNT FSPCMs had a relative high thermal performance at a relatively low cost by employing CITs as supporting material compared to other existing PCMs used for low-temperature applications, such as capric-myristic acid/vermiculite/expanded graphite, Capric acid-LA/gypsum, paraffin/kaolin, propyl palmitate/gypsum, capric acid–palmitic acid/gypsum wallboard, xylitol pentalaurate/gypsum, palmitic acid/active aluminum oxide, and so on. Therefore, the prepared LA/CIT/CNT FSPCMs have a potential for TES application to be employed as building materials or decorative materials at low temperature, for example, in geothermal heating and low-temperature waste heat utilization. Particularly, it has a significant potential for the fabrication of different novel construction building materials, such as brick, cement, concrete, wallboard, and plaster used for building energy conservation, emission reduction, and temperature regulation.

Table 4. Thermal properties between the fabricated samples and reported by the literature.

Item (wt%)	Melting Temperature (°C)	Solidifying Temperature (°C)	Latent Heat of Melting (J/g)	Latent Heat of Solidifying (J/g)	References
Capric-myristic acid (20)/vermiculite + expanded graphite (2)	19.7	17.1	26.9	missing	[39]
Capric acid-lauric acid (26)/gypsum	19.11	missing	35.24	missing	[40]
Paraffin(18)/kaolin	23.9	26.3	27.9	missing	[41]
Propyl palmitate(25–30)/gypsun	19.0	16.0	40.0	missing	[42]
Capric acid-Palmitic acid (25)/gypsum wallboard	21.12	21.46	36.23	38.28	[43]
Xylitol pentalaurate (20)/gypsum	40.44	39.53	31.77	29.47	[44]
Palmitic acid (25)/active aluminum oxide	74.13	59.57	28.56	17.53	[45]
LA (27.5)/CIT	45.8	39.39	45.06	38.73	This study
LA (27.5)/CIT/CNT (3)	45.24	39.61	39.95	35.63	This study

3.5. Thermal Reliability of LA/CIT/CNT FSPCM

In addition, the thermal reliability of the prepared LA/CIT/CNT FSPCM was evaluated using a cyclic test. And the thermal stability of the LA/CIT/CNT FSPCM samples after 120 thermal cycles was tested by DSC. The performance of the LA/CIT/CNT FSPCM sample before and after heating and cooling cycles is shown in Figure 7. As seen in Figure 7, after 120 thermal cycles, the melting temperature and freezing temperature of the LA/CIT/CNT FSPCMs were increased by 0.1 °C and 0.78 °C, respectively, and the latent heat for the melting process and the freezing process was slightly reduced by 1.78% and 4.63%, respectively. The latent heat of the LA/CIT/CNT FSPCMs was slightly lower after heating and cooling cycles, and the phase-change temperature showed a slight deviation after the repeated heating and cooling cycles. This may be due to the appearance of imperfect crystallites with the addition of CITs or CNTs [46,47]. No degradation was observed during the repeated heating and cooling cycles. This was because the DSC temperature of the measured LA/CIT/CNT FSPCM was about 60 °C, which was lower than the initial degradation temperatures of LA/CIT/CNT FSPCMs. Comparing the DSC results of the LA/CIT/CNT FSPCMs before and after heating and cooling cycles, there was no significant difference in the phase-change temperature and latent heat value during the melting and solidifying processes. After 120 thermal cycles, the latent heat of LA/CIT/CNT FSPCM during the melting process can be maintained at a reasonable level. Though they experienced a long life cycle, the LA/CIT/CNT FSPCMs still demonstrated good thermal reliability. The special structure of CITs and CNTs imparted FSPCMs with good thermal reliability reflected by a slight variation in latent heat.

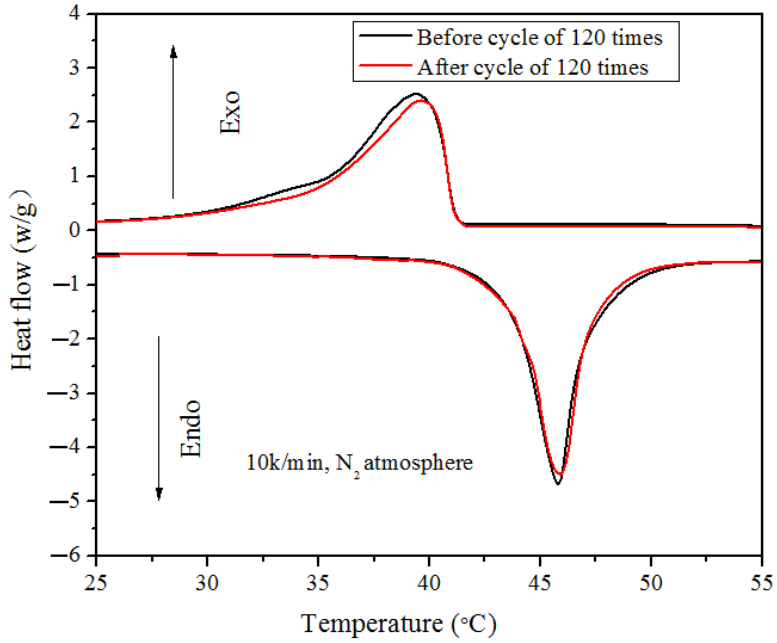

Figure 7. DSC cures of LA/CIT/CNT FSPCM before and after 120 cycles.

3.6. Thermal Stability of the FSPCMs

Figure 8 showed the thermal stability of the FSPCMs. As illustrated in Figure 8, the initial degradation temperatures of LA and the LA/CIT FSPCMs and LA/CIT/CNT FSPCMs were about 125 °C. The initial degradation temperatures of the prepared FSPCMs were all higher than their working temperature of 39–46 °C. No decomposition of the LA/CIT/CNT FSPCMs occurred within the range from room temperature to the initial decomposition temperature, meaning that the LA/CIT/CNT FSPCMs had good thermal stability during the range of its working temperature. In addition, the weight loss of the prepared FSPCMs was about 24.17% and 21.2%, respectively, which is almost consistent with the percentages of LA adsorbed in the FSPCMs. The TGA results indicated the LA/CIT/CNT FSPCMs had good thermal stability under the working temperature.

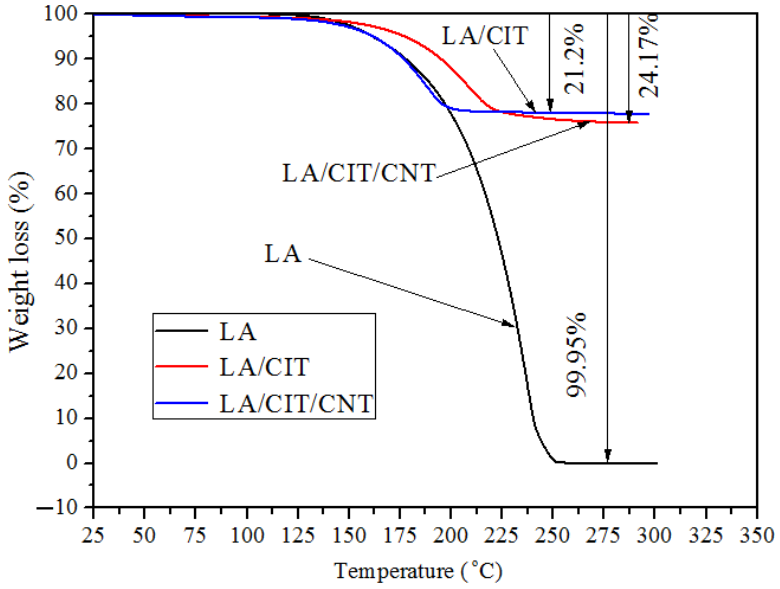

Figure 8. TGA cures of LA, LA/CIT FSPCMs, and LA/CIT/CNT FSPCMs.

3.7. Heat Transfer Efficiency of the FSPCMs

The measured heat storage/release results of the samples were presented in Figure 9 and Table 5 to assess the heat transfer efficiency. As can be seen from Figure 9 and Table 5, it required about 12 min for pure LA to reach the melting point from 25 °C, whereas it required only 11 min and 10.5 min for the LA/CIT FSPCMs and LA/CIT/CNT FSPCMs to reach to their melting point, respectively. In the solidifying process, it required about 6 min for the pure LA to reach the solidification point, whereas it required only 5 min and 3 min for the LA/CIT FSPCMs and LA/CIT/CNT FSPCMs to reach their solidification point from 75 °C, respectively. Moreover, the constant equilibrium temperature time of the LA/CIT/CNT FSPCMs was about 4.5 min during the melting process and 3 min during the solidification process, respectively, while it required 5 min and 5 min for the LA/CIT FSPCMs, and 23 min and 6 min for LA. These fully confirmed that the heat transfer efficiency of the LA/CIT/CNT FSPCMs was enhanced due to the introduction of the CNT additive. In other words, the thermal storage/release rate was significantly improved. The heat transfer efficiency of the LA/CIT/CNT FSPCMs showed obvious advantage over others, which was 84.62% higher than LA and 50% higher than the LA/CIT FSPCMs during the freezing process, respectively. The abovementioned analysis meant that the addition of CNTs can improve the heat transfer efficiency of FSPCMs during heat absorption and release.

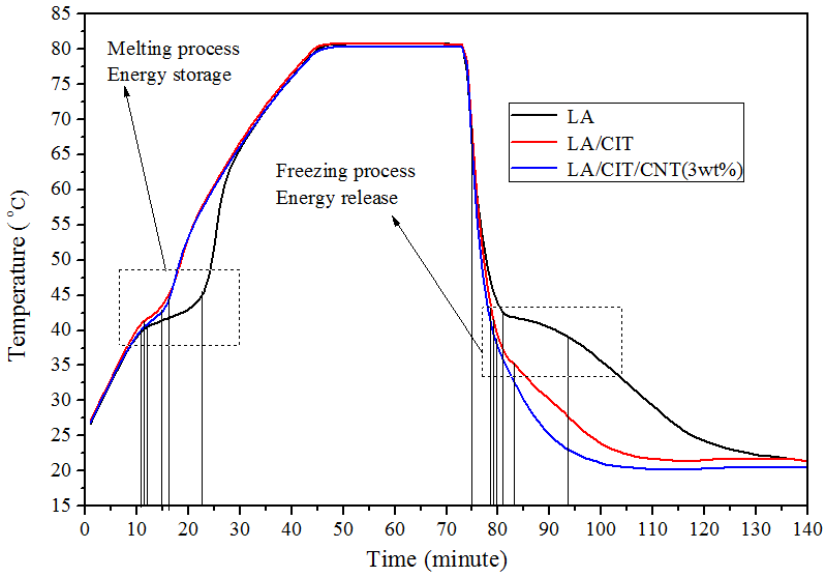

Figure 9. Storage and release curves of LA, LA/CIT FSPCMs, and LA/CIT/CNT FSPCMs.

Table 5. Comparisons of performance parameters and heat transfer rate among the prepared samples.

Sample	Heat Time (min)	Heat Storing Time (min)	Freezing Time (min)	Heat Releasing Time (min)	Improved Heat Rate (%)	Improved Freezing Rate (%)
LA	12	23	6	13	—	—
LA/CIT	11	5	5	4	78.26	69.23
LA/CIT/CNT	10.5	4.5	3	2	80.43	84.62

The improvement mechanism of the heat transfer efficiency of the LA/CIT/CNT FSPCMs by the addition of CNTs can be contributed to the self-high thermal conductivity of CNTs. The CNT additive was dispersed and fully mixed with LA and CITs, which could provide a large heat transfer area and greatly reduce heat resistance. Meanwhile, when thermal energy was considered as the energy wave, CNTs could greatly reduce the wave resistance during the heat transfer process. Moreover, CNTs can change the direction of the energy wave across the LA on the surface of the micro-porous structure of the CITs.

Thus, the addition of CNTs could enhance the heat transfer channels of LA and increase the thermal conductivity by coupling LA and CITs with its self-high thermal conductivity [2].

4. Conclusions

In this work, a novel FSPCM was prepared via a simple direct impregnation method, where LA was chosen as a PCM to store thermal energy, CITs were used as a supporting matrix to prevent the leakage of LA during phase-change transition, and CNTs were selected as the thermal conductivity additive. Based on the above discussion, the main conclusions can be drawn as follows.

(1) The leakage test results and SEM analysis results indicated that CITs can be employed as a supporting matrix for preventing leakage of LA. Moreover, when the mass fraction of LA retained in the composite was 27.5%, the LA/CIT/CNT FSPCM was formed without the leakage of LA.
(2) The FTIR showed there were no chemical reactions among the three components, namely, LA, CITs, and CNTs of the FSPCMs. The results of TGA demonstrated that the thermal stability of the LA/CIT/CNT FSPCMs at their working temperature was satisfactory.
(3) The LA/CIT/CNT FSPCMs melted at 45.24 °C with a latent heat of 39.95 J/g and solidified at 39.61 °C with a latent heat of 35.63 J/g, respectively. Through the repeated heating and cooling cycles, the LA/CIT/CNT FSPCMs had good thermal reliability.
(4) Compared with pure LA, the thermal transfer efficiency of the LA/CIT/CNT FSPCMs were significantly improved with the addition of CNTs. The thermal transfer efficiency of the LA/CIT/CNT FSPCMs was improved by 80.43% for the melting process and 84.62% for the solidification process than those of LA.

Therefore, through the above analysis, it was shown that the LA/CIT/CNT FSPCMs have relatively superior properties with low preparation cost, which shows that it has potential for storing and releasing thermal energy in practical applications for low-temperature TES. In a word, LA/CIT/CNT FSPCMs can improve the comprehensive utilization of ITs. Moreover, it has a significant potential to fabricate new different construction materials to be used in energy-saving buildings.

Author Contributions: Conceptualization, P.L. and Y.W.; methodology, P.L. and Y.W.; investigation, P.L. and J.R.; resources, S.J., J.R., Z.L. and Z.Z.; writing—original draft preparation, P.L. and Y.W.; writing—review and editing, P.L. and Z.Z.; supervision, Z.Z. and Z.L.; project administration, Z.Z. and Z.L.; funding acquisition, Y.W. All authors have read and agreed to the published version of the manuscript.

Funding: This research was funded by by Key R&D Projects of Tibet Autonomous Region Science and Technology Program (XZ202101ZY0008G), the Science and Technology Project of Hebei Education Department (ZD2022053), the Key Technology R&D Program of Hebei Province (17214016), the Funding Projects that guide local for scientific and technological development of Hebei Provincial Department of Science and Technology (236Z4504G), and the Open Foundation of Hebei Key Laboratory of Green Development of Rock and Mineral Materials (RM202310). And the APC was funded by [XZ202101ZY0008G], or [236Z4504G) and [RM202310]. Meanwhile, we are grateful to Xue Yin for her help during the sample preparation experiments.

Data Availability Statement: All data generated or analyzed during this study were included in this published article.

Conflicts of Interest: The authors declare no competing financial interests.

References

1. Liu, P.; Gu, X.B.; Bian, L. Enhanced thermal conductivity of palmitic acid/mullite phase change composite with graphite powder for thermal energy storage. *Renew. Energ.* **2019**, *138*, 833–841.
2. Sun, M.Y.; Liu, T.; Sha, H.N.; Li, M.L.; Liu, T.Z.; Wang, X.L.; Chen, G.J.; Wang, J.D.; Jiang, D.Y. A review on thermal energy storage with eutectic phase change materials: Fundamentals and applications. *J. Energy Storage* **2023**, *68*, 107713.

3. Adesusi, O.M.; Adetunji, O.R.; Kuye, S.I.; Musa, A.I.; Erinle, T.J.; Gbadamosi-Olatunde, O.B.; Ipadeola, S.O. A comprehensive review of the materials degradation phenomena in solid-liquid phase change materials for thermal energy storage. *Int. J. Thermofluids* **2023**, *18*, 100360.
4. Liu, P.; Gu, X.B.; Bian, L.; Cheng, X.F.; Peng, L.H.; He, H.C. Thermal properties and enhanced thermal conductivity of capric acid/diatomite/Carbon nanotubes composite as form-stable phase change materials for thermal energy storage. *ACS Omega* **2019**, *4*, 2964–2972. [CrossRef]
5. Zhang, H.J.; Zhang, X.G.; Pan, D.; Ai, Y.H.; Chen, Y.S. Preparation and application of high-temperature composite phase change materials. *J. Energy Storage* **2023**, *68*, 107669.
6. Luo, L.X.; Luo, W.X.; Chen, W.J.; Hu, X.W.; Ma, Y.; Xiao, S.K.; Li, Q.l.; Jiang, X.G. Form-stable phase change materials based on graphene-doped PVA aerogel achieving effective solar energy photothermal conversion and storage. *Sol. Energy* **2023**, *255*, 146–156. [CrossRef]
7. Khademi, A.; Mehrjardi Seyed, A.A.; Said, Z.; Saidur, R.; Ushak, S.; Chamkha Ali, J. A comparative study of melting behavior of phase change material with direct fluid contact and container inclination. *Energy Nexus* **2023**, *10*, 100196.
8. Kumar, N.; Rathore Pushpendra, K.S.; Sharma, R.K.; Gupta Naveen, K. Integration of lauric acid/zeolite/graphite as shape stabilized composite phase change material in gypsum for enhanced thermal energy storage in buildings. *Appl. Therm. Eng.* **2023**, *224*, 120088. [CrossRef]
9. Wu, M.M.; Liu, C.Z.; Rao, Z.H. Preparation and performance of lauric acid phase change material with the double-layer structure for solar energy storage. *J. Energy Storage* **2023**, *65*, 107385. [CrossRef]
10. Karaipekli, A.; Biçer, A.; Sarı, A.; Tyagi, V. Thermal characteristics of expanded perlite/paraffin composite phase change material with enhanced thermal conductivity using carbon nanotubes. *Energy Convers. Manag.* **2017**, *134*, 373–381. [CrossRef]
11. Lin, J.H.; Ouyang, Y.X.; Chen, L.; Wen, K.; Li, Y.; Mu, H.Z.; Ren, Q.L.; Xie, X.Z.; Long, J.Y. Enhancing the solar absorption capacity of expanded graphite-paraffin wax composite phase change materials by introducing carbon nanotubes additives. *Surf. Interfaces* **2022**, *30*, 101871. [CrossRef]
12. Ramakrishnan, S.; Wang, X.; Sanjayan, J. Thermal enhancement of paraffin/hydrophobic expanded perlite granular phase change composite using graphene nanoplatelets. *Energy Build.* **2018**, *169*, 206–215. [CrossRef]
13. Zhou, D.Y.; Xiao, S.Z.; Xiao, X.H. Preparation and Thermal Performance of Fatty Acid Binary Eutectic Mixture/Expanded Graphite Composites as Form-Stable Phase Change Materials for Thermal Energy Storage. *ACS Omega* **2023**, *8*, 8596–8604. [CrossRef] [PubMed]
14. Fan, Z.X.; Zhao, Y.C.; Ding, Y.F.; Shi, Y.; Liu, X.Y.; Jiang, D.H. Fabrication and comprehensive analysis of expanded perlite impregnated with myristic acid-based phase change materials as composite materials for building thermal management. *J. Energy Storage* **2022**, *55*, 105710. [CrossRef]
15. Liu, X.Y.; Zhao, Y.C.; Fan, Z.X.; Shi, Y.; Jiang, D.H. Preparation and characterization of lauric acid–stearic acid/expanded perlite as a composite phase change material. *RSC Adv.* **2022**, *12*, 23860–23868. [CrossRef]
16. Sarı, A. Fabrication and thermal characterization of kaolin-based composite phase change materials for latent heat storage in buildings. *Energy Build.* **2015**, *96*, 193–200. [CrossRef]
17. Jafaripour, M.; Sadrameli, S.M.; Pahlavanzadeh, H.; Mousavi, S.S. Fabrication and optimization of kaolin/stearic acid composite as a form-stable phase change material for application in the thermal energy storage systems. *J. Energy Storage* **2021**, *33*, 102155.
18. Ren, M.; Zhao, H.; Gao, X.J. Effect of modified diatomite based shape-stabilized phase change materials on multiphysics characteristics of thermal storage mortar. *Energy* **2022**, *241*, 122823. [CrossRef]
19. Jia, W.B.; Wang, C.M.; Wang, T.J.; Cai, Z.Y.; Chen, K. Preparation and performances of palmitic acid/diatomite form-stable composite phase change materials. *Int. J. Energ. Res.* **2020**, *44*, 4298–4308. [CrossRef]
20. Wang, H.; Rao, Z.H.; Li, L.Q.; Liao, S.M. A novel composite phase change material of high-density polyethylene/d-mannitol/expanded graphite for medium-temperature thermal energy storage: Characterization and thermal properties. *J Energy Storage* **2023**, *60*, 106603.
21. Liang, Z.k.; Peng, X.; Huang, Z.C.; Li, J.Y.; Yi, L.Y.; Huang, B.Y.; Chen, C.Z. Innovative methodology for comprehensive utilization of refractory low-grade iron ores. *Powder Technol.* **2023**, *418*, 118283.
22. Li, C.; Sun, H.H.; Bai, J.; Li, L.T. Innovative methodology for comprehensive utilization of iron ore tailings: Part 1. The recovery of iron from iron ore tailings using magnetic separation after magnetizing roasting. *J. Hazard. Mater.* **2010**, *174*, 71–77. [CrossRef] [PubMed]
23. Rao, G.V.; Markandeya, R.; Sharma, S.K. Recovery of Iron Values from Iron Ore Slimes of Donimalai Tailing Dam Recovery of Iron Values from Iron Ore Slimes of Donimalai Tailing Dam. *Trans. Indian Inst. Met.* **2016**, *69*, 143–150. [CrossRef]
24. Lv, P.Z.; Liu, C.Z.; Rao, Z.H. Review on clay mineral-based form-stable phase change materials: Preparation, characterization and applications. *Renew. Sust. Energ. Rev.* **2017**, *68*, 707–726.
25. Sobolciak, P.; Karkri, M.; Al-Maadeed, M.; Krupa, I. Thermal characterization of phase change materials based on linear low-density polyethylene, paraffin wax and expanded graphite. *Renew. Energ.* **2016**, *88*, 372–382. [CrossRef]
26. Liu, S.; Han, L.; Xie, S.; Jia, Y.; Sun, J.; Jing, Y.; Zhang, Q. A novel medium-temperature form-stable phase change material based on dicarboxylic acid eutectic mixture/expanded graphite composites. *Sol. Energy* **2017**, *143*, 22–30. [CrossRef]
27. Karaipekli, A.; Sarı, A. Preparation, thermal properties and thermal reliability of eutectic mixtures of fatty acids/expanded vermiculite as novel form-stable composites for energy storage. *J. Ind. Eng. Chem.* **2010**, *16*, 767–773.

28. Jeong, S.; Jeon, J.; Chung, O.; Kim, S.; Kim, S. Evaluation of PCM/diatomite composites using exfoliated graphite nanoplatelets (xGnP) to improve thermal properties. *J. Therm. Anal. Calorim.* **2013**, *114*, 689–698. [CrossRef]
29. Deng, Y.; Li, J.H.; Qian, T.T.; Guan, W.M.; Wang, X. Preparation and characterization of KNO_3/diatomite shape-stabilized composite phase change material for high temperature thermal energy storage. *J. Mater. Sci. Technol.* **2016**, *33*, 198–203. [CrossRef]
30. Li, M.; Guo, Q.G.; Nutt, S. Carbon nanotube/paraffin/montmorillonite composite phase change material for thermal energy storage. *Sol. Energy* **2017**, *146*, 1–7. [CrossRef]
31. Liu, P.; Gu, X.B.; Zhang, Z.K.; Shi, J.P.; Rao, J.; Bian, L. Fabrication and Thermal Properties of Capric Acid/Calcinated Iron Tailings/Carbon Nanotubes Composite as Form-Stable Phase Change Materials for Thermal Energy Storage. *Minerals* **2019**, *9*, 648. [CrossRef]
32. Gu, X.B.; Liu, P.; Bian, L.; Peng, L.H.; Liu, Y.G.; He, H.C. Mullite Stabilized Palmitic Acid as Phase Change Materials for Thermal Energy Storage. *Minerals* **2018**, *8*, 440–450. [CrossRef]
33. Liu, P.; Zhang, Z.K.; Gu, X.B.; Rao, J.; Shi, J.P.; Bian, L. Fabrication of a novel shape-stabilized composite phase change material based on multivariate supporting materials by using typical solid wastes. *Constr. Build. Mater.* **2020**, *240*, 118156. [CrossRef]
34. Lv, P.Z.; Liu, C.Z.; Rao, Z.H. Experiment study on the thermal properties of paraffin/kaolin thermal energy storage form-stable phase change materials. *Appl. Energ.* **2016**, *182*, 475–487.
35. Liu, P.; Gu, X.B.; Bian, L.; Peng, L.H.; He, H.C. Capric acid/intercalated diatomite as form-stable composite phase change material for thermal energy storage. *J. Therm. Anal. Calorim.* **2019**, *138*, 359–368.
36. Ramakrishnan, S.; Wang, X.; Sanjayan, J.; Wilson, J. Assessing the feasibility of integrating form-stable phase change material composites with cementitious composites and prevention of pcm leakage. *Mater. Lett.* **2017**, *192*, 88–91. [CrossRef]
37. Feng, Y.; Wei, R.; Huang, Z.; Zhang, X.; Wang, G. Thermal properties of lauric acid filled in carbon nanotubes as shape-stabilized phase change materials. *Phys. Chem. Chem. Phys.* **2018**, *20*, 7772–7780.
38. Shen, Q.; Ouyang, J.; Zhang, Y.; Yang, H. Lauric acid/modified sepiolite composite as a form-stable phase change material for thermal energy storage. *Appl. Clay Sci.* **2017**, *146*, 14–22.
39. Karaipekli, A.; Sari, A. Capric–myristic acid/vermiculite composite as form-stable phase change material for thermal energy storage. *Sol. Energy* **2009**, *83*, 323–332. [CrossRef]
40. Shilei, L.; Neng, Z.; Guohui, F. Eutectic mixtures of capric acid and lauric acid applied in building wallboards for heat energy storage. *Energy Build.* **2006**, *38*, 708–711. [CrossRef]
41. Memon, S.; Liao, W.; Yang, S.; Cui, H.; Shah, S. Development of composite PCMs by incorporation of paraffin into various building materials. *Materials* **2015**, *8*, 499–518. [CrossRef] [PubMed]
42. Karaman, S.; Karaipekli, A.; Sari, A.; Bicer, A. Polyethylene glycol (peg)/diatomite composite as a novel form-stable phase change material for thermal energy storage. *Sol. Energy Mater. Sol. Cells* **2011**, *95*, 1647–1653.
43. Sari, A.; Karaipekli, A.; Kaygusuz, K. Capric acid and myristic acid for latent heat thermal energy storage. *Energ Source Part A* **2008**, *30*, 1498–1507. [CrossRef]
44. Biçer, A.; Sarı, A. New kinds of energy-storing building composite PCMs for thermal energy storage. *Energy Convers. Manag.* **2013**, *69*, 148–156.
45. Fang, G.; Li, H.; Cao, L.; Shan, F. Preparation and thermal properties of form-stable palmitic acid/active aluminum oxide composites as phase change materials for latent heat storage. *Mater. Chem. Phys.* **2012**, *137*, 558–564. [CrossRef]
46. Jiang, L.; Liu, Z.; Yuan, Y.; Wang, Y.; Lei, J.; Zhou, C. Fabrication and characterization of fatty acid/wood-flour composites as novel form-stable phase change materials for thermal energy storage. *Energy Build.* **2018**, *171*, 88–99.
47. Zhang, X.; Fan, Y.; Tao, X.; Yick, K. Crystallization and prevention of supercooling of microencapsulated n-alkanes. *J. Colloid Interf. Sci.* **2005**, *281*, 299–306. [CrossRef]